Chemical Engineering Journal 156 (2010) 270–277

Contents lists available at ScienceDirect

Chemical Engineering Journal

journal homepage: www.elsevier.com/locate/cej

Molded micro- and mesoporous carbon/silica composite from rice husk and beet sugar

Seiji Kumagai [a,*], Hirotaka Ishizawa [a], Yuta Aoki [a], Yasuhiro Toida [b]

[a] Department of Machine Intelligence and Systems Engineering, Akita Prefectural University, Tsuchiya-aza-ebinokuchi 84-4, Yurihonjo 015-0055, Japan
[b] Petroleum Refining Research and Technology Center, Japan Energy Corporation, Niizominami 3-17-35, Toda 335-8502, Japan

ARTICLE INFO

Article history:
Received 15 May 2009
Received in revised form
26 September 2009
Accepted 6 October 2009

Keywords:
Activated carbon
Composite
Rice husk
Silica
Porosity
Briquette

ABSTRACT

A molded carbon/silica composite with high micro- and mesoporosity, as well as a high bulk density, was fabricated by activating a disk-molded precursor made from carbonized rice husk (RH) and beet sugar (BS) at 875 °C in CO_2. The pore structure of the RH- and BS-based carbon/silica composite (RBC) was analysed in relation to the bulk density. An activation time of 2.0 h provided the largest BET specific surface area (1027 m^2/g) and total pore volume (0.68 cm^3/g) and a low bulk density (0.54 g/cm^3). An RBC that was first activated for 1 h was immersed again in BS syrup and then activated in CO_2 for 1 h. This two-step activation process provided both a high bulk density (0.69 g/cm^3) and a highly textured structure (BET specific surface area, 943 m^2/g; total pore volume, 0.56 cm^3/g). The immersion in BS syrup was useful for improving the texture without reducing the bulk density, in comparison to one-step activation for 1.0 h. The suspension of the RBCs was basic because of the residual inorganic compounds of potassium and calcium. However, the basicity of the suspension was alleviated by washing the RBCs with water.

1. Introduction

The utilization of agricultural by-products promotes efficient waste management and reduces usage of petroleum and mining products, thus contributing to environmental conservation. Rice is a staple food in Japan and 10.9 million metric tons were produced in 2004 [1]. About 2 million metric tons of rice husks (RHs) are produced annually in Japan as an agricultural by-product of rice threshing [2]. The most common method for disposing of RHs in Japan used to be incineration on the farm. However, this is now discouraged because it produces ash, fumes, and toxic organic gases, leading to serious air pollution. At present, 63 mass% of RHs produced in Japan is used in the agricultural, livestock, energy (fuel) and material engineering industries, but the rest is not dealt with efficiently [2].

The failure to make use of all of the RHs is due, in part, to the double layer composed of silica and cuticle that resists invasion by insects and pathogenic organisms. This protective layer slows natural biodegradation, which discourages the re-utilization of RHs in the agricultural and livestock industries. The ash content of RHs, which is mostly silica, is approximately 20 mass%. This high ash content means that the carbon content is low, limiting the use of RHs as a fuel source or as a precursor for the production of carbon-based materials. However, RHs do have a noteworthy advantage. Most of the rice harvested in Japan is threshed in integrated large-scale facilities, and a large quantity of RHs can be collected at low cost. It would be socially and industrially beneficial if these RHs were recycled.

The industrial importance of porous materials such as activated carbon (AC) is well known, especially for processes such as separation, purification, catalysis and electrolysis, which require a highly porous structure [3]. There have been many attempts to produce RH-based porous materials by means of physical activation [4–6] and chemical activation [7–9]. A characteristic of RH-based porous material is the simultaneous appearance of micro- and mesoporosity resulting from the carbon and the silica content, respectively [10]. The Brunauer–Emmett–Teller (BET) specific surface area (SSA) of RH-based porous materials produced by physical (CO_2 gas) activation is ~500 m^2/g [6], whereas that generated by chemical activation using KOH and NaOH is ~3000 m^2/g [9]. Yeletsky et al. recently obtained RH-based mesoporous carbon by leaching out the silica by the use of K_2CO_3 and Na_2CO_3 at 750–1000 °C [11]. Deiana et al. produced RH-based carbon, with an SSA of 700–1200 m^2/g after the ash ingredients were leached out by HF [12].

A higher bulk density is required to increase the adsorption performance of ACs in a specified volume in applications such as fixed-bed reactor columns. The above-mentioned RH-based porous materials are basically powders. However, it is difficult for ACs to attain both a highly textured structure and a high bulk density. Pendyal et al. described the bulk density and the textural proper-

* Corresponding author. Tel.: +81 184 27 2128; fax: +81 184 27 2128.
E-mail address: kumagai@akita-pu.ac.jp (S. Kumagai).

1385-8947/$ – see front matter © 2009 Elsevier B.V. All rights reserved.
doi:10.1016/j.cej.2009.10.016

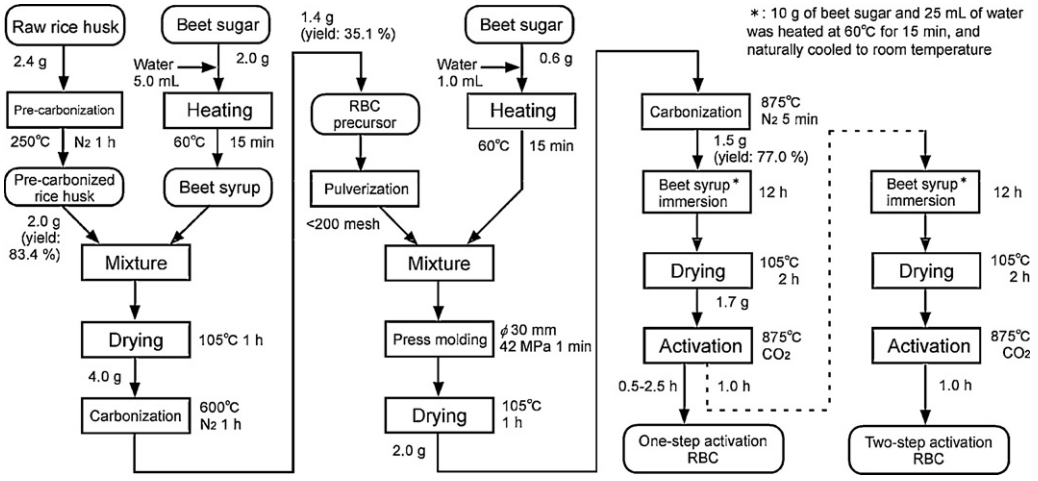

Fig. 1. A process to fabricate molded RBCs.

ties of granular ACs produced from RHs and several types of binder [4]. They showed that a sugar-based binder (a mass ratio of binder to RH of 1:1) was more useful than the conventional coal tar binder and improved both texture and bulk density. An AC made from RHs and a sugar-based binder completely derived from crops would seem to be ideal for separation and purification processes requiring extremely high levels of safety. Sugarcane and sugar beet are major sugar crops in Japan. The annual yield of beet sugar (BS) in Japan is about 4.3 million metric tons, which is three times greater than that of sugarcane [13].

Because of the intrinsic silica in raw RHs, heating in an inert condition can produce a natural carbon/silica composite structure. In addition to this, RH-based porous materials with micro- and mesoporosity can be produced. In this study, an attempt was made to produce a molded RH- and BS-based carbon/silica composite (RBC), with a high level of micro- and mesoporous structure as well as with a high bulk density, by using BS syrup as a binder.

2. Materials and methods

2.1. Fabrication method of RBC

The RH sample was obtained by threshing Koshihikari rice harvested in Toyooka, Iwata City, Japan in autumn 2004. The raw RH was air-dried at 105 °C for 3 h. The BS was supplied by the Hokuren Agriculture Cooperative Association (Hokkaido, Japan).

The carbonization process was done in an electric furnace (KT-1053R; Advantec Toyo, Japan). The sample was heated from room temperature to the desired carbonization temperature in 1 h at a constant heating rate in a flow (700 mL/min) of N_2. The sample was kept at this temperature for the desired length of time and then allowed to cool to room temperature. For the activation process, the disk-molded sample was heated to 875 °C in 1 h at a constant heating rate in a flow (700 mL/min) of N_2. Then the gas was changed to CO_2 (700 mL/min) and the sample was maintained at 875 °C for the desired length of time. Finally, the sample was allowed to cool to room temperature in a flow of CO_2. The flow rates of N_2 and CO_2 (700 mL/min) were used to attain highly inert activation conditions and to minimize the effects of gases emitted from the sample.

Fig. 1 shows the one-step activation process used for fabrication of the RBC. BS that had been carbonized at 250 °C was added in the form of syrup to the RHs. The blend was heated at 600 °C and then pulverized. The powder obtained was press-molded into a disk using the BS syrup as a binder. The molded disk was heated at 875 °C and then immersed in BS syrup. The disk was dried and then activated at 875 °C in CO_2 for 0.5–2.5 h. A two-step activation was also used to produce both a highly porous structure and a high bulk density. The bulk density was calculated by measuring the mass, the diameter and the thickness of the fabricated disk, and the mass yields of the one-step and two-step activations were calculated. The RBC produced by one-step activation in 1.0 h was named RBC1.0. Using the same system, RBC2.5 signifies an RBC produced by one-step activation for 2.5 h and the RBC created by two-step activation was named RBC1.0 + 1.0.

Fig. 2 shows photographs of the raw RH activated at 875 °C for 1 h, the BS syrup activated at 875 °C for 1 h, the RH ash, and the RBC1.0. The RH ash was produced by heating the raw RH in an air flow (700 mL/min) at 875 °C for 1 h. Except for RBC1.0, the samples were very fragile and pulverable. The activated BS syrup was like an inflated balloon. The photographs show that simply activating RH or BS syrup alone did not create a dense porous material. A gradual addition of BS syrup into several states of the RBC was useful to prevent inflation of the BS syrup and to fabricate a dense RBC.

2.2. Textural characterization

Nitrogen adsorption–desorption isotherms at −196 °C were obtained using a gas adsorption analyser (Autosorb-3B; Quantachrome Instruments Inc., USA). The disk-shaped RBCs were crushed into granules of ~1 mm diameter for measurement of the nitrogen adsorption–desorption isotherm. The other samples were not processed mechanically or chemically for that measurement. A sample of 0.02 g was degassed at 200 °C for >3 h before the isotherm measurement. The BET SSA (S_{BET}) is based on the BET theory and was calculated using the volume of N_2 adsorbed at relative pressures of 0.05–0.1 [3]. The liquid N_2 volume in relation to the N_2 volume adsorbed at relative pressure 0.995 was determined as the total pore volume (V_t). Microporosity in ACs was essentially slit-shaped [14,15]. The formation of micropores in lignocellulosic raw materials such as wood, coconut shell, etc. probably arose from a mechanism involving the transformation of lignocellulose into carbon polyhexagon sheets (graphenes) [15]. Slit-shaped pores were assumed for the microporosity produced in carbonaceous structures in the RBCs. In the present study, micropores were distinguished as either ultramicropores (width ≤0.7 nm) or supermicropores (0.7 < width ≤ 2.0 nm), in accordance with Sing et al. [16]. The pore size distribution was evaluated using density functional theory (DFT) [17,18]. The DFT method is applicable to the whole range of micro- and mesopores using a single numerical data reduction [19], which was suitable for the pore size analy-

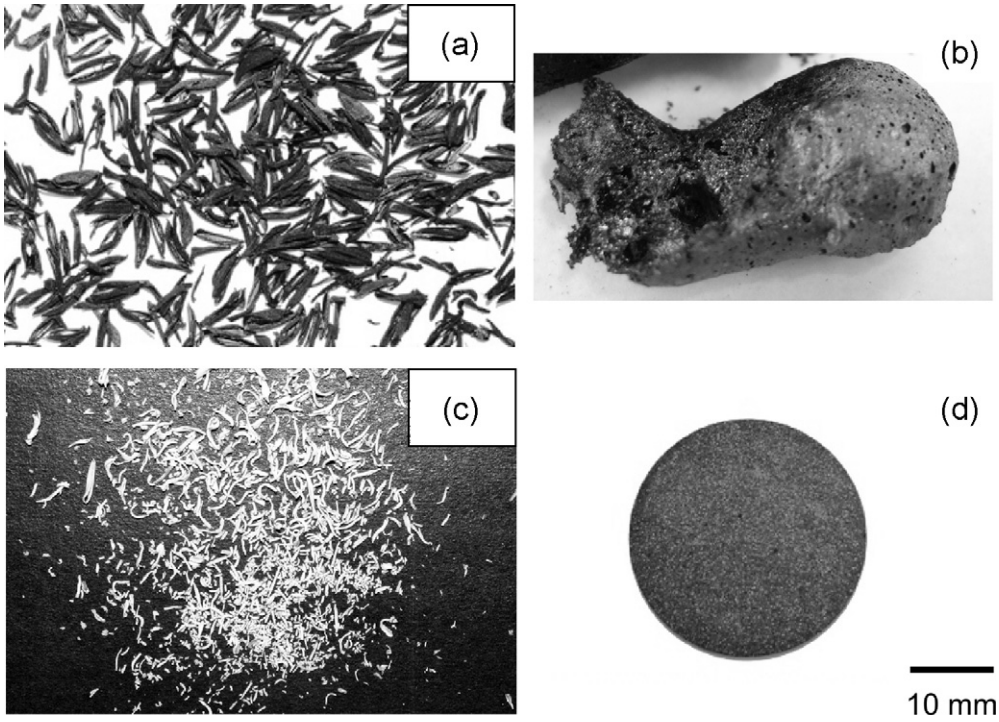

Fig. 2. Photos of the treated source materials and the RBC1.0. (a) Raw RH activated at 875 °C for 1 h, (b) BS syrup activated at 875 °C for 1 h, (c) RH ash and (d) RBC1.0.

sis of the micro- and mesoporous RBCs fabricated in this study. The DFT software developed by Quantachrome Instruments Inc. (version 1.62) was used to obtain the distribution of pore size. The volumes of ultramicropores (V_u), supermicropores (V_s), and mesopores (V_m) were obtained using these pore size distribution data. The macropore volume (V_c) was calculated as follows:

$$V_c = V_t - (V_u + V_s + V_m)$$

where V_{micro} is the volume of micropores and equals $V_u + V_s$.

2.3. Compositional analysis

The ash content of 0.1 g samples was determined from the residual ash after incineration at 800 °C for 1 h in an air flow (100 mL/min) using a thermogravimetric analyser (TGA-51; Shimadzu Corp., Japan). The composition of the raw RH ash was determined using a fluorescent X-ray analyser (XRF-1700, Shimadzu Corp., Japan). A CHN/S analyser (2400 I; PerkinElmer Inc., USA) was used to determine the hydrogen, carbon, nitrogen and sulfur content of the samples. The oxygen content, excluding that in the ash, was determined as the mass minus the hydrogen, carbon, nitrogen, sulfur, and ash. Because oxygen might be added with inorganic matter during the ashing, the oxygen content might be in error. All samples were dried at 105 °C for 3 h before analysis. It was verified beforehand that this length of time was sufficient to yield a constant weight on drying.

2.4. X-ray diffractometry

X-ray diffraction (XRD) patterns were obtained in order to investigate the crystallinity of the RBCs. The RBC was pulverized to <200 mesh. An X-ray diffractometer (CuKα, X'Pert Pro; PANalytical, Japan) was used, in which the X-ray output conditions were set as 45 kV and 40 mA.

2.5. Evaluation of acidity and basicity

The acidity and basicity of the RBC surface were determined as the pH of the suspension. The Boehm titration method was used for evaluating the acidity and basicity of the sample surface [20]. The suspension was prepared by adding 1 g of the pulverized RBC (<200 mesh) into 100 mL of distilled water. The glass vessel containing the suspension was sealed and then shaken for 24 h at 25 °C, then the pH of the filtered suspension was measured. In addition to this, 1 g of the pulverized RBC was immersed in 100 mL of 0.1 mol/L NaOH or 100 mL of 0.1 mol/L HCl. The glass vessel containing the solution and the RBC was sealed and then shaken for 24 h at 25 °C. The excess basicity or acidity of the filtered solutions (50 mL) was titrated with HCl or NaOH, respectively. The numbers of acidic and basic sites were calculated from the amount of HCl and NaOH consumed by the titration, respectively.

3. Results and discussion

3.1. Textural properties of RBCs fabricated under different conditions

Typical nitrogen adsorption–desorption isotherms of the fabricated RBCs at −196 °C are shown in Fig. 3. The sharp knees at relative pressure <0.1 were observed for all samples and are typical of micropore systems. A gradual increase in the isotherm slope at relative pressures >0.1 and a hysteresis loop at a high relative pressure, indicating the existence of mesopores, were observed for all samples. The hysteresis loops had no sharp knee, meaning that mesopores of specific sizes were absent. The isotherms of all the RBCs belong to type IV as classified by IUPAC [16]. The isotherms of the RBCs processed by one-step activation at low relative pressure (<0.1) increased for activation times up to 1.5 h and decreased with longer activation times. The greatest nitrogen uptake at relative pressure 0.995 was observed for RBC2.0, indicating that the activation time of 2.0 h provided the largest total pore volume. The isotherm slope at a high relative pressure (>0.5) increased with acti-

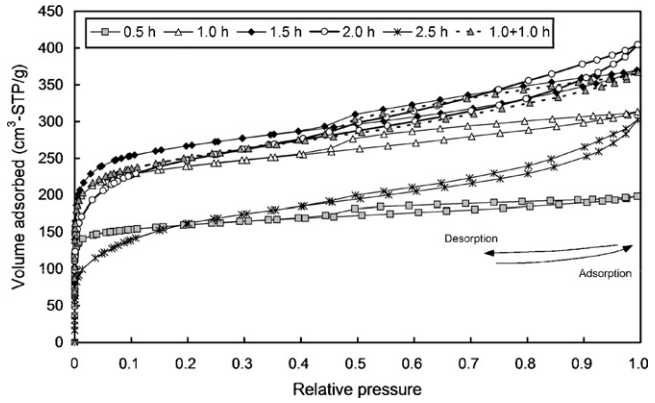

Fig. 3. Typical nitrogen adsorption–desorption isotherms of the RBCs produced by one-step activation for 0.5–2.5 h and two-step activation for 1.0 + 1.0 h at −196 °C.

vation time, showing that the longer activation process developed the meso- and macropores. The isotherm of the RBC produced using the two-step activation process (RBC1.0 + 1.0) was analogous to that of RBC1.0 at lower relative pressure (<0.1) and was analogous to that of RBC1.5 at higher relative pressure (>0.7).

Fig. 4 shows the nitrogen adsorption–desorption isotherms at −196 °C of raw RH activated at 875 °C for 1 h, BS syrup activated at 875 °C for 1 h, RH ash, and RBC1.0. The isotherm of activated BS syrup showed a typical isotherm of type I as classified by IUPAC [16], indicating that the activated BS syrup was highly microporous. The shapes of the isotherms of RBC1.0 and activated raw RH are analogous. The differences between them were the nitrogen uptake at very low relative pressure (<0.05) and the size of the hysteresis loops. Thus, the higher degree of micro- and mesoporosity of RBC1.0 were attributed to carbon deposition impregnated from the BS syrup. A low-pressure hysteresis was observed on the isotherm of RH ash, which was type H3 as classified by IUPAC, suggesting the presence of slit-shaped pores [16]. No nitrogen uptake at relative pressures ≤0.1, and smaller nitrogen uptake and hysteresis loop at relative pressures >0.1 on the isotherm of the RH ash implies that it formed no microporosity and scanty mesoporosity with slit-shaped pores, producing a template of porosity of RBCs and activated raw RH. Mesoporosity of RBC1.0 and activated raw RH was attributed to carbon deposition on the inorganic template, which resulted from the intrinsic lignocellulosic content of both the raw RH and the added BS syrup. Thus, micro- and mesopores in the RBC samples was assumed to be slit-shaped pores.

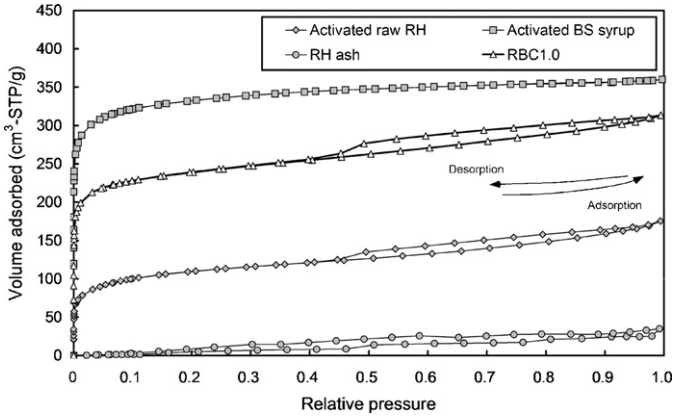

Fig. 4. Nitrogen adsorption–desorption isotherms at −196 °C of the raw RH activated at 875 °C for 1 h, the BS syrup activated at 875 °C for 1 h, the RH ash, and the RBC1.0.

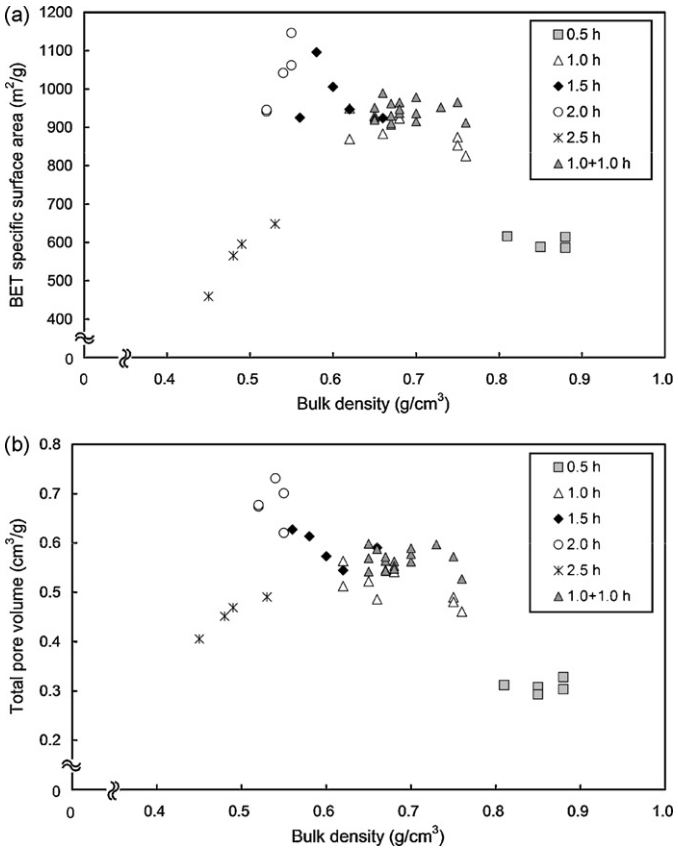

Fig. 5. BET specific surface area and total pore volume of the RBCs produced by one-step activation for 0.5–2.5 h and two-step activation for 1.0 + 1.0 h as a function of the bulk density. (a) BET specific surface area and (b) total pore volume.

The BET SSA and the total pore volume of the RBCs are plotted as a function of the bulk density in Fig. 5. The BET SSA and the total pore volume of the RBCs prepared using one-step activation for 0.5–2.0 h increased as the bulk density decreased. Activation for >2.0 h decreased the BET SSA and the total pore volume. The RBC prepared using two-step activation (RBC1.0 + 1.0) displayed a larger BET SSA and a larger total pore volume than that prepared by one-step activation (RBC1.0), at a bulk density of 0.65–0.75 g/cm^3.

Fig. 6 shows the DFT pore size distributions of all RBCs, which were calculated on the basis of the nitrogen adsorption–desorption isotherms shown in Fig. 3. A carbon slit pore equilibrium model was used to obtain the DFT pore size distributions because micro- and mesopores produced in the RBC samples can be treated as slit-shaped pores with carbonaceous walls. The volume of supermicropores, of width 1.0–2.0 nm, increased with activation time up to 2.0 h. No significant difference was observed between the pattern of pore size distribution in RBCs produced by one-step activation (1.0 h) or by two-step activation (1.0 + 1.0 h).

The volumes of the ultramicro-, supermicro-, meso- and macropores of the RBCs, which were calculated from the results of the DFT pore size distributions, were evaluated as a function of bulk density (see Fig. 7). The volume of ultramicropores of the RBCs produced by one-step activation was maintained at a bulk density of 0.7–0.9 g/cm^3 and decreased for bulk densities <0.7 g/cm^3. The ultramicropore volume of the RBCs produced by one-step and by two-step activation were very similar. The volumes of supermicro- and mesopores were greater in the lower part of the bulk density range (0.5–0.9 g/cm^3) and showed decreased values at 0.4–0.5 g/cm^3. RBC1.0 produced by one-step activation and RBC1.0 + 1.0 produced by two-step activation were in the similar bulk density range of 0.60–0.75 g/cm^3. Student's *t*-test showed

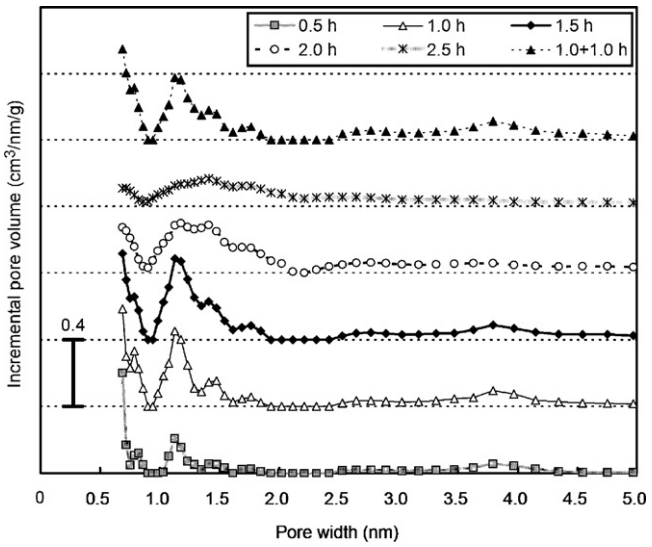

Fig. 6. DFT pore size distributions of the RBCs produced by one-step activation for 0.5–2.5 h and two-step activation for 1.0 + 1.0 h.

that the average mesopore volume of RBC1.0 + 1.0 was significantly larger ($P < 0.05$) than that of RBC1.0. Table 1 summarizes the textural properties of the RBCs and the mass yield of the activation.

3.2. Chemical properties of RBCs

Table 2 gives the elemental composition of some RBCs. The carbon and hydrogen contents of RBC produced by one-step activation decreased with activation time and the ash content increased. RBC0.5 had a greater hydrogen content, indicating that an activation time of 0.5 h was too brief to release the hydrogen bonded to the RH and BS. The two-step activation process, which includes one more immersion in BS syrup, resulted in a greater carbon content and a smaller ash content of RBC1.0 + 1.0 compared to RBC2.0 subjected to the same total activation time. The carbon and the ash contents of RBC2.0 were both 48 mass%. Fluorescent X-ray analysis of the ash produced from the raw RH found that the major component was SiO_2 (86.8 mass%), with K_2O (8.0 mass%), CaO (2.0 mass%) and P_2O_5 (1.1 mass%) among other materials.

Fig. 8 shows the XRD patterns of the RBCs. The peak or halo at 22°, which developed with activation time, was attributed to the cristobalite structure of silica [21], which seems to be related to crystallization occurring with longer activation times. A very weak peak was observed at 26° on the XRD patterns of RBS1.0 + 1.0 and

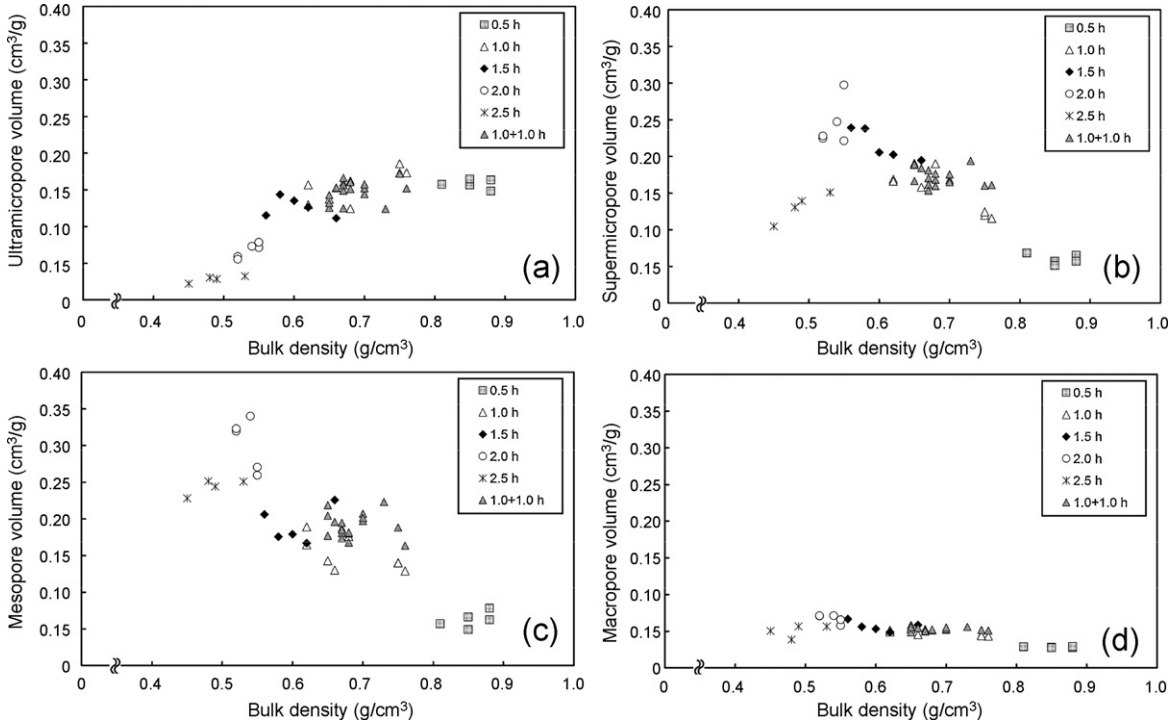

Fig. 7. Volumes of pores, divided into four types, in the RBCs produced by one-step activation for 0.5–2.5 h and two-step activation for 1.0 + 1.0 h as a function of the bulk density: (a) ultramicropores, (b) supermicropores, (c) mesopores and (d) macropores.

Table 1
Textural properties of the RBCs produced by one-step activation for 0.5–2.5 h and two-step activation for 1.0 + 1.0 h, and the mass yield of the activation.

Sample	BD (g/cm³)	S_{BET} (m²/g)	V_t (cm³/g)	V_u (cm³/g)	V_s (cm³/g)	V_m (cm³/g)	V_c (cm³/g)	Yield[a] (mass%)
RBC0.5	0.85	599	0.31	0.16	0.06	0.06	0.03	74.0
RBC1.0	0.69	889	0.51	0.15	0.15	0.15	0.06	54.8
RBC1.5	0.60	978	0.59	0.13	0.22	0.19	0.06	47.6
RBC2.0	0.54	1027	0.68	0.07	0.24	0.30	0.07	32.5
RBC2.5	0.49	564	0.45	0.03	0.13	0.24	0.05	26.5
RBC1.0 + 1.0	0.69	943	0.56	0.15	0.17	0.19	0.05	61.4[b]

BD means bulk density.
[a] 100 mass% = the mass of the RBC after the first beet syrup immersion and drying.
[b] 100 mass% = the mass of the RBC after the second beet syrup immersion and drying.

Table 2
Composition of RBCs produced using one-step activation for 0.5 and 2.0 h and two-step activation for 1.0 + 1.0 h.

Sample	C (mass%)	H (mass%)	N (mass%)	S (mass%)	Ash (mass%)	O (diff) (mass%)
RBC0.5	68.06	0.16	0.45	0.01	29.32	2.00
RBC2.0	48.37	0.02	0.65	0.03	48.45	2.48
RBC1.0 + 1.0	58.60	0.03	0.55	0.01	36.83	3.98

Data are the averages of four separate measurements. Oxygen content, except for that in ash, was calculated as: O = 100 − (Ash + H + C + N + S).

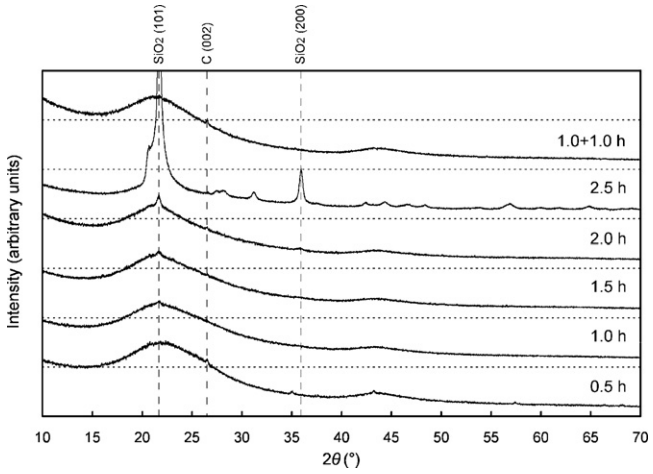

Fig. 8. XRD patterns of the RBCs produced by one-step activation (0.5–2.5 h) and two-step activation (1.0 + 1.0 h).

RBC0.5, which both had a large carbon content. This peak might be due to micro-graphite structures on the pore walls [22], but was too weak to be identified with certainty. The results of the compositional and X-ray diffraction analysis described above indicated that a composite structure of carbon/silica was produced in the RBCs.

Table 3
pH and numbers of surface acidic and basic sites on the RBCs.

Sample	pH	Total acidic sites (mmol/g)	Total basic sites (mmol/g)
RBC0.5	9.5	0.99	0.16
RBC2.0	9.5	0.69	0.30
RBC1.0 + 1.0	9.5	0.96	0.18

Data are the results of single measurements.

The acidity and basicity of the RBC surfaces were evaluated by measurement of pH and titration of the suspension. Table 3 gives the surface pH and the numbers of surface acidic and basic sites. The suspension made by adding the RBCs to distilled water was basic (pH 9.5), which was attributed to the potassium and calcium components in the ash of raw RH. It was found that more acidic sites than basic sites were produced on the surfaces of all RBCs. It was noted that RBC2.0, which was subjected to a longer one-step activation process, showed an increased ratio of basic sites to acidic sites, in comparison to RBC0.5. This was attributed to the longer activation time leading to the loss of carbon and the increased content of basic potassium and calcium ingredients. The surface property of RBC1.0 + 1.0 was more similar to that of RBC0.5 than that of RBC2.0, although the total activation times for RBC2.0 and RBC1.0 + 1.0 were similar. The additional immersion in BS syrup that was used for RBC1.0 + 1.0 restricted the loss of carbon and the formation of basic sites. The suspension was filtered, the residual RBCs were recov-

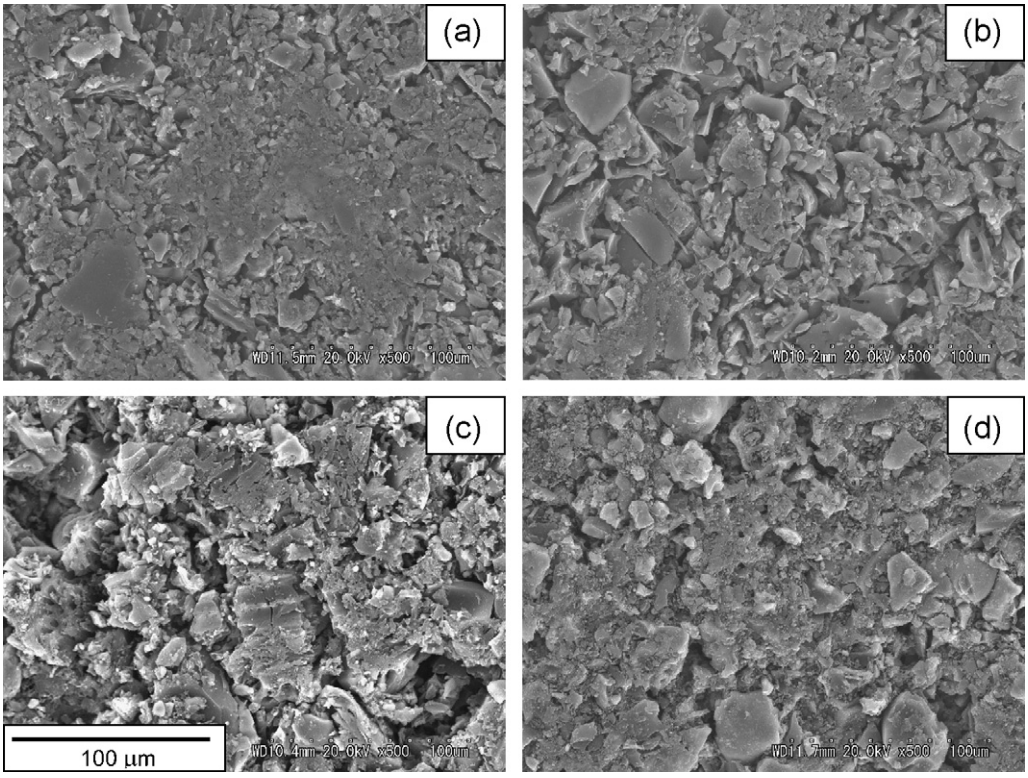

Fig. 9. Scanning electron micrographs of the RBC surfaces. (a) RBC0.5, (b) RBC1.0, (c) RBC2.0 and (d) RBC1.0 + 1.0.

Table 4
The bulk density and textural properties of RH-based porous materials produced under gas activation (from the literature), compared with results for RBC 1.0 + 1.0.

Sample	BD (g/cm^3)	S_{BET} (m^2/g)	V_t (cm^3/g)	V_{micro} (cm^3/g)	Reference
RBC1.0 + 1.0	0.69	943	0.56	0.32	Present study
RH and sugar syrup based granular AC	0.35[a]	350	–	–	[4]
RH based silica/carbon porous composite	0.45	450	–	–	[23]
RH and grape must based AC briquette	–	386	–	0.148	[5]

BD: Bulk density. –: No data.
[a] Filling density in a graduated cylinder.

ered and dried, and a suspension of these was prepared as 0.8 g of RBC in 80 mL of distilled water. The pH of these suspensions was ~8, indicating that basic ingredients had leached into the water. Therefore, a washing process might be required for RBC samples intended for use in water treatments.

3.3. Characteristics of RBCs

The surface appearance of the RBC samples was observed in a scanning electron microscope (SEM-EDX Integration System, Hitachi, Ltd., Japan). Fig. 9 shows the scanning electron micrographs of the RBCs. The surface of the RBC produced by one-step activation (RBC0.5, RBC1.0 and RBC2.0) was found to allow more and larger cracks with increasing activation time, revealing that the activation process involved a disappearance of carbon, resulting in a reduction of the bulk density. For RBC1.0 + 1.0 produced by two-step activation, smaller and fewer cracks were observed on the surface when compared to RBC1.0 and RBC2.0. The filling of cracks on RBC1.0 + 1.0 was likely to be accomplished by one more immersion in BS syrup before the second activation.

RBCs with high micro- and mesoporosity, as well as a high bulk density, were fabricated by using RH and BS. The BS used in the form of syrup had three roles. The first was to provide carbon source to RH in order to develop its pore structure. The second was a binder to mold the char produced by heating the mixture of RH and BS into a pressed disk. The third was to increase the density of the RBC. The sample was immersed in BS syrup before the activation process, which contributed to filling cracks in the sample with carbon derived from BS.

Gradual addition of BS syrup to several states of the RBC prevented an inflation of the BS syrup during its carbonization and its activation, finally attaining both high bulk density and porosity. Micro- and mesoporosity of the RBCs, which were more developed than those of the activated raw RH, were shown to result from carbon deposition from the BS syrup. The results of the textural characterization and compositional analysis suggested that the RBCs formed a silica/carbon composite with a very wide distribution of pore size (ultramicro- to macropore).

In addition to this, altering the activation conditions could change the distribution of pore size. The ultramicropores degenerated, whereas supermicro- and mesopores were developed with increasing activation time of up to 2.0 h. The bulk density and the activation yield of the RBC produced by one-step activation decreased with activation time. The results given in Table 2 show that the carbon content decreased and the ash content increased with increased activation time. Thus, the activation process ablated slit-shaped pores with carbonaceous walls in the RBCs, which increased their supermicro- and mesopore volumes, and decreased their ultramicropore volume and bulk density. Further activation for 2.5 h ablated the pores excessively, which reduced all of the textural properties. Thus, activation for 2.5 h was not beneficial because it resulted in the lowest bulk density, textural properties and yield.

From the viewpoint of attaining both a highly textured structure and a high bulk density, RBC1.5 and RBC2.0 allowed excessive activation and were not suitable. When compared to one-step activation for 1.0 h, the two-step activation process resulted in larger mesopore volume, leading to a larger total pore volume, at comparable micropore volume and bulk density. Therefore, RBC1.0 + 1.0 was judged to be the most promising material for attaining both great textural property and high bulk density in the fabricated RBC samples.

The properties of other RH-based porous materials for which density and textural information have been reported are given in Table 4 and compared with those of RBC1.0 + 1.0. It should be noted that the fabrication processes of the materials shown in Table 4 were different from that of the RBC1.0 + 1.0. This demonstrates clearly that RBC1.0 + 1.0 had a greater bulk density and texture than the previous RH-based porous materials produced under gas activation. More acidic sites than basic sites were produced on all RBCs. The suspension of the RBCs was basic because of residual inorganic compounds of potassium and calcium. However, the basicity of the suspension can be alleviated by washing the RBCs with water. With a high bulk density and large mesopore volume, liquid-phase adsorption in a specified volume, such as water treatment using a fixed-bed reactor, is one of the potential applications of the RBCs.

4. Conclusions

Micro- and mesoporous carbon/silica composites were made from the agricultural by-product RH, using BS as a binder, by means of CO_2 gas activation. The relationship between the textural properties and the bulk density was studied. A two-step activation process, which included a second immersion in BS syrup, was shown to be useful for developing mesopores in the RBC without reducing the bulk density, in comparison to a one-step activation process. As a molded AC, RBC1.0 + 1.0 produced by two-step activation had high bulk density (0.69 g/cm^3), sufficient micropore volume (0.32 cm^3/g) and large mesopore volume (0.19 cm^3/g). This displayed a higher bulk density and greater textural properties than those of the RH-based porous materials reported earlier.

Acknowledgements

This research was supported in part by the Industrial Technology Research Grant Program in 2006 of the New Energy and Industrial Technology Development Organization (NEDO) of Japan. We are grateful to Dr. Teruo Bito of Akita Prefectural University, and Dr. Y. Enda and Miss K. Sato of the Akita Research and Development Center for their help with instrumental analyses.

References

[1] Food and Agricultural Organization of the United Nations, FAOSTAT, 2006, http://faostat.fao.org/.
[2] New Energy and Industrial Technology Development Organization, Estimated Amount of Existent and Available Biomass in Japan: GIS Database, 2006, http://app1.infoc.nedo.go.jp/kinds/no2.pdf (in Japanese).
[3] R.C. Bansal, M. Goyal, Activated Carbon Adsorption, CRC Press Inc., Boca Raton, FL, USA, 2005.
[4] B. Pendyal, M.M. Johns, W.E. Marshall, M. Ahmedna, R.M. Rao, The effect of binders and agricultural by-products on physical and chemical properties of granular activated carbons, Bioresour. Technol. 68 (1999) 247–254.

[5] A. Amaya, N. Medero, N. Tancredi, H. Siva, C. Deiana, Activated carbon briquettes from biomass materials, Bioresour. Technol. 97 (2007) 1635–1641.
[6] S. Kumagai, K. Sasaki, Y. Shimizu, K. Takeda, Formaldehyde and acetaldehyde adsorption properties of heat-treated rice husks, Sep. Purif. Technol. 61 (2008) 398–403.
[7] Y. Guo, K. Yu, Z. Wang, H. Xu, Effects of activation conditions on preparation of porous carbon from rice husk, Carbon 41 (2000) 1645–1687.
[8] N. Yalcin, V. Sevinc, Studies of the surface area and porosity of activated carbons prepared from rice husks, Carbon 38 (2000) 1943–1945.
[9] Y. Guo, S. Yang, K. Yu, J. Zhao, Z. Wang, H. Xu, Adsorption of Cr(VI) on micro- and mesoporous rice husk-based active carbon, Mater. Chem. Phys. 74 (2002) 320–323.
[10] T.H. Liou, Evolution of chemistry and morphology during the carbonization and combustion of rice husk, Carbon 42 (2004) 785–794.
[11] P.M. Yeletsky, V.A. Yakovlev, M.S. Mel'gunov, V.N. Parmon, Synthesis of mesoporous carbons by leaching out natural silica templates of rice husk, Micropor. Mesopor. Mater. 121 (2009) 34–40.
[12] C. Deiana, D. Granados, R. Venturini, A. Amaya, M. Sergio, N. Tancredi, Activated carbons obtained from rice husk: Influence of leaching on textural parameters, Ind. Eng. Chem. Res. 47 (2008) 4754–4757.
[13] Ministry of Agriculture, Forestry and Fisheries of Japan, Statics of Agriculture, Forestry and Fisheries: Industrial Crops, 2008, http://www.maff.go.jp/www/info/bunrui/mono04.html (in Japanese).
[14] H. Marsh, F. Rodriguez-Reinoso, Activated Carbon, Elsevier Ltd., Oxford, UK, 2006.
[15] A. Albornoz, M. Labady, M. Lopez, J. Laine, Evidence for the formation of slit mesopores in activated carbon, J. Mater. Sci. Lett. 18 (1999) 1999–2000.
[16] K.S.W. Sing, D.H. Everett, R.A.W. Haul, L. Moscou, R.A. Pierotti, J. Rouquerol, T. Siemieniewska, Reporting physisorption data for gas/solid systems, Pure Appl. Chem. 57 (1985) 603–619.
[17] J.P. Olivier, Improving the models used for calculating the size distribution of micropore volume of activated carbons from adsorption data, Carbon 36 (1998) 1469–1472.
[18] Z. Ryu, J. Zheng, M. Wang, B. Zhang, Characterization of pore size distributions on carbonaceous adsorbent by DFT, Carbon 37 (1999) 1257–1264.
[19] International Organization for Standardization, ISO 15901-3, Pore size distribution and porosity of solid materials by mercury porosimetry and gas adsorption—Part 3: analysis of micropores by gas adsorption, 2007.
[20] H.P. Boehm, Surface oxides on carbon and their analysis: a critical assessment, Carbon 40 (2002) 145–149.
[21] International Center for Diffraction Data, Powder Diffraction File, SiO_2 (Cristobalite) 27–605, 208, 1986.
[22] The Carbon Society of Japan, Shin tanso zairyo nyumon [An introduction to new carbon materials], REALIZE Inc., Tokyo, Japan, 2000 (in Japanese).
[23] T. Watari, A. Nakata, Y. Kiba, T. Torikai, M. Yada, Fabrication of porous SiO_2/C composite from rice husks, J. Eur. Ceram. Soc. 26 (2006) 797–801.